

## Research Highlights

- The Zerilli-Armstrong model was modified to account for the diffusion processes
- The softening effects of DRV and DRX were integrated into the flow stress equation
- A physically-based constitutive model was proposed for predicting hot flow curves

ACCEPTED MANUSCRIPT

# A Simple Zerilli-Armstrong Constitutive Equation for Modeling and Prediction of Hot Deformation Flow Stress of Steels

Tina Mirzaie <sup>a</sup>, Hamed Mirzadeh <sup>a,\*</sup>, Jose-Maria Cabrera <sup>b,c</sup>

<sup>a</sup> School of Metallurgy and Materials Engineering, College of Engineering, University of Tehran, P.O. Box 11155-4563, Tehran, Iran

<sup>b</sup> Departamento de Ciencia de los Materiales e Ingeniería Metalúrgica, ETSEIB, Universitat Politècnica de Catalunya, Av. Diagonal 647, 08028 Barcelona, Spain

<sup>c</sup> Fundació CTM Centre Tecnològic, Pl. de la Ciència, 08243, Manresa, Spain

## Abstract

Generally, the dislocation-mechanics-based constitutive relations are applicable at high strain rates and relatively low temperatures. However, for expressing flow stress at elevated temperatures, it is required to account for the diffusion processes, namely softening effects of dynamic recovery (DRV) and dynamic recrystallization (DRX). In the current work, the Zerilli-Armstrong constitutive equation for face-centered cubic materials was appropriately modified by incorporation of peak strain and consideration of both hardening and softening phenomena. The developed constitutive relation was successfully applied to model the hot flow stress of a typical carbon steel and it was revealed that there is no need to alter the physically-based nature of the Zerilli-Armstrong constitutive equation by extensive modifications.

**Keywords:** Thermomechanical processing; Constitutive modeling; Hot working; Dynamic recrystallization.

---

\* Corresponding author. Tel.: +982182084127; Fax: +982188006076.  
E-mail address: hmirzadeh@ut.ac.ir (H. Mirzadeh).

## 1. Introduction

Hot working is an important step in production of materials with required shape, microstructure, and mechanical properties (Doherty et al., 1997; Mirzadeh et al., 2011a; Mirzadeh et al., 2011b; Mirzadeh and Najafizadeh, 2013). Since the computer simulation of metal forming processes is used increasingly in the industry and any feasible mathematical simulation needs accurate flow description, a proper flow stress model is a preliminary requirement. As a result, considerable research has been carried out to model the flow stress of metals and alloys (Anand, 1985; Ahmed et al., 2005; Brown et al., 1989; Lin and Chen, 2011; Luo et al., 2010; Mirzadeh, 2014a; Mirzadeh, 2015a; Mirzadeh, 2015b; Parsa and Ohadi, 2013; Sun et al., 2010; Zhang et al., 2009; Samantaray et al., 2009; Cai et al., 2015; Chai et al., 2012). Johnson and Cook (1983) proposed the most common constitutive equation by consideration of the effects of strain, strain rate, and deformation temperature, separately. This uncoupled nature is a main problem of the Johnson-Cook model, especially for flow stress modeling at elevated temperatures (Akbari et al., 2015; Mirzadeh, 2015c). On the other hand, Zerilli and Armstrong (1987) proposed dislocation-mechanics-based constitutive relations for different crystalline structures, in which the effects of strain hardening, strain rate hardening, and thermal softening based on the thermal activation analysis were incorporated into constitutive relations. For fcc metals, the Zerilli-Armstrong (ZA) model can be expressed as  $\sigma = c_0 + B_0 \varepsilon^{0.5} \exp(-\beta_0 T + \beta_1 T \ln \dot{\varepsilon})$  (Zerilli and Armstrong, 1987; Zerilli, 2004), in which  $c_0$  and  $B_0$  have the unit of MPa and  $\beta_0$  and  $\beta_1$  have the unit of  $\text{K}^{-1}$ . The constant  $c_0$  as the athermal term adds the influence of solutes and grain boundaries to the thermal stress term. The ZA model can be modified as  $\sigma = c_0 + B_0 \varepsilon^n \exp(-\beta_0 T + \beta_1 T \ln \dot{\varepsilon})$ , in

which the use of a power law strain hardening with a power of  $n$  instead of 0.5 is an attempt to better account for the effects of dynamic recovery (DRV) and the consequent saturation of the stress-strain curve at large strains (Zerilli, 2004).

The ZA equation should be expected to apply at high strain rates and relatively low temperatures ( $T < 0.5T_m$ ) (Zerilli and Armstrong, 1987). One of the important characteristics of deformation at elevated temperatures is the simultaneous occurrence of DRV and dynamic recrystallization (DRX), which are the restoration phenomena that significantly affect the flow stress (Mirzadeh 2015a; Mirzadeh and Najafizadeh, 2010; Saadatkia et al., 2015). Moreover, since the diffusion processes are enhanced at high temperatures, the deformation mechanism is normally controlled by the intragranular glide and climb of dislocations (Mirzadeh et al., 2011a; Mirzadeh, 2015d; Mirzadeh et al., 2015). Therefore, the flow stress is not greatly affected by the initial grain size (Mirzadeh, 2015e; Mukherjee, 2002; Langdon, 2005), and hence, the term  $c_0$  can be neglected. Furthermore, the strain rate sensitivity is high at hot working temperatures, which shows that the thermally-activated dislocation glide becomes much more prominent. In the current study, the ZA model was evaluated for a plain carbon steel at elevated temperatures and subsequently modified to make it useful for modeling the hot deformation flow curves.

## 2. Experimental details

Uniaxial hot compression tests were performed on cylindrical samples of a 0.50C-0.68Mn-0.20Si-0.28Cu steel with the height of 11.4 mm and diameter of 7.6 mm. The strain rate and temperature for this work were in the range of  $0.0001-0.1 \text{ s}^{-1}$  and 900-1100

°C, respectively. Samples were soaked at 1100 °C for 15 min before the compression test and argon flow was employed to inhibit decarburization of the specimen and oxidation of the machine tools. More information about the experiments and preliminary hot deformation behaviors can be found elsewhere (Escobar et al., 2003; Saadatkia et al., 2015) and are here revisited.

### **3. Results and discussion**

#### *3.1. Flow behavior*

The obtained flow curves are shown in Fig. 1. Most of the curves illustrate the conventional DRX behavior (Dehghan-Manshadi et al., 2008; Mirzadeh, 2014b, Mirzadeh et al., 2012), showing a broad peak with subsequent flow softening. During initial stages of deformation the dislocation multiplication and interaction result in an increase in the flow stress, during which dynamic recovery is underway. After the dislocation density reaches a critical value, aided by a relatively slow DRV kinetics, the DRX becomes operative promoting a strong additional softening which is reflected in the form of a peak stress in the flow curve. Afterward, a flow softening region appears and continues till reaching a steady state stress. Figure 1 also shows that the flow stress increases by increasing strain rate and decreasing deformation temperature, and hence, the effect of temperature and strain rate is significant and should be appropriately incorporated into the flow stress formula.

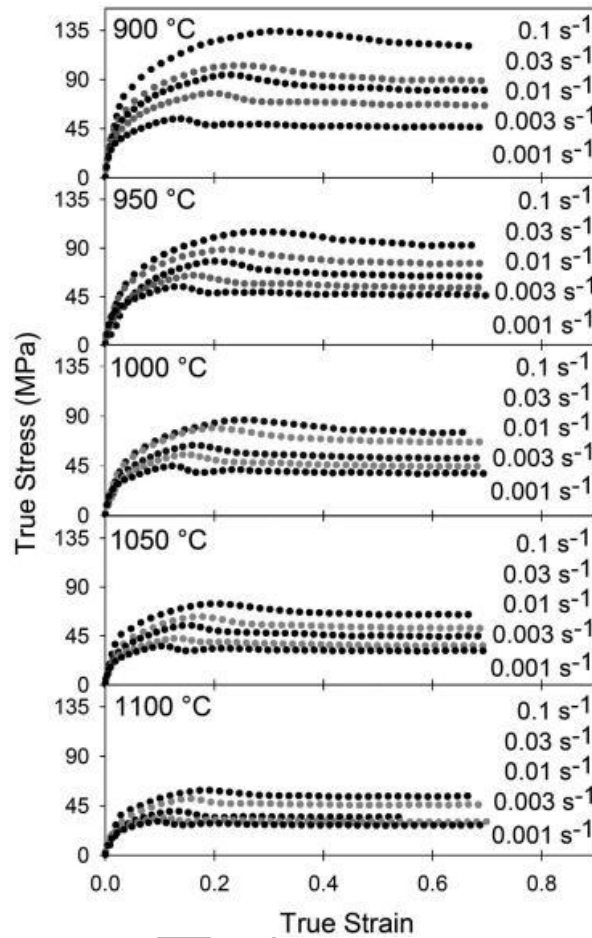


Fig. 1: Obtained flow curves at different deformation conditions.

### 3.2. The original ZA model with $n=0.5$

By neglecting the term  $c_0$  and taking natural logarithm from both sides of the original Zerilli-Armstrong (ZA) model (Zerilli and Armstrong, 1987; Zerilli, 2004), the relation  $\ln \sigma = \ln B_0 + 0.5 \ln \varepsilon - (\beta_0 - \beta_1 \ln \dot{\varepsilon})T$  is obtained. For calculating the appropriate value of  $B_0$ , a reference strain rate of  $0.03 \text{ s}^{-1}$  was considered. As a result,  $B_1 = \beta_0 - \beta_1 \ln \dot{\varepsilon}$  becomes a constant. It follows from the above expression that the slope of the plot of  $\ln \sigma$  against  $T$  at a constant strain can be used to obtain the value of  $B_1$  at a specific strain. The required plot is shown in Fig. 2a, which shows that the lines for different

strains are nearly parallel, and hence,  $B_1$  does not depend on strain and the average value of  $B_1=0.00344 \text{ K}^{-1}$  was taken for subsequent analysis.

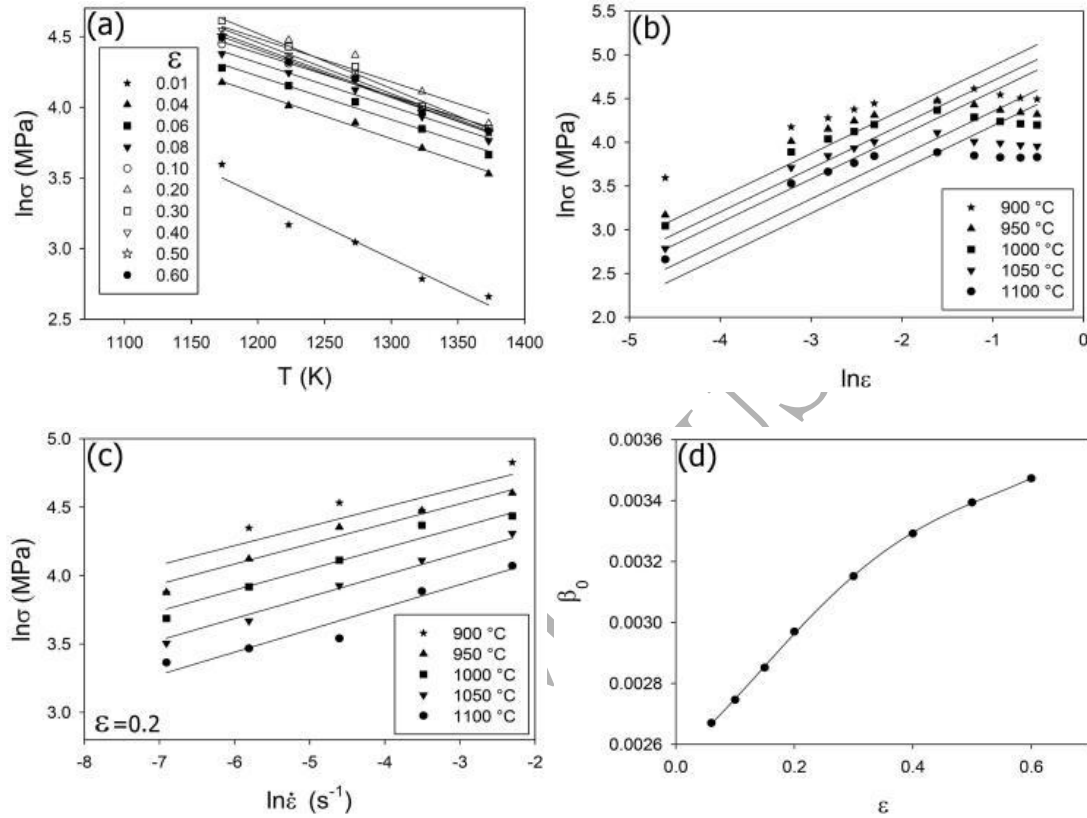


Fig. 2: Plots used to find the constants of the original ZA model.

Based on the above analysis, the ZA equation can be simplified as  $\ln \sigma = (\ln B_0 - 0.00344T) + 0.5 \ln \epsilon$ . It follows that the intercept of the plot of  $\ln \sigma$  vs.  $\ln \epsilon$  by fitting lines with slope of 0.5 ( $y = 0.5x + b$ ) at a constant temperature can be used to obtain the value of  $\ln B_0 - 0.00344T$  at that specific temperature. This is shown in Fig. 2b and it was found that  $B_0$  does not depend on temperature and its average value was determined as  $B_0 = 11697.5 \text{ MPa}$ . Besides the above analysis, it can be deduced from Fig.

2b that two slopes with different signs are required to represent the data. This fact will be revisited later for modification of the ZA model in Section 3.6.

For calculating  $\beta_0$  and  $\beta_1$ , the ZA equation can be expressed as

$$\sigma = 11697.5\varepsilon^{0.5} \exp(-\beta_0 T + \beta_1 T \ln \dot{\varepsilon}) \quad \text{or} \quad \ln \sigma = \{\ln(11697.5\varepsilon^{0.5}) - \beta_0 T\} + \beta_1 T \ln \dot{\varepsilon}.$$

Therefore, at a given strain (in the interval of 0.06 to 0.6), the slopes and the intercepts of the plots of  $\ln \sigma$  vs.  $\ln \dot{\varepsilon}$  at different temperatures can be used to obtain the average values of  $\beta_0$  and  $\beta_1$ . A representative plot (for strain of 0.2) is shown in Fig. 2c. It was found that the value of  $\beta_1$  does not depend considerably on strain and its value can be taken as  $0.00012 \text{ K}^{-1}$ . The average value of  $\beta_0$  was also taken as  $0.003069 \text{ K}^{-1}$ . However, while  $\beta_0$  should be a constant in the original ZA model, it can be seen in Fig. 2d that it depends somehow on strain. Based on the above analyses, the ZA equation can be expressed as follows:

$$\sigma = 11697.5\varepsilon^{0.5} \exp(-0.003069T + 0.00012T \ln \dot{\varepsilon}) \quad (1)$$

Fig. 3 shows the comparison between the experimental and calculated flow stress for some representative curves using Eq. 1. As it is apparent, the original ZA model cannot adequately predict the flow curves at hot working conditions. Despite the visual examination, the ability of the model can be better evaluated by calculating the root mean square error (RMSE) and the percentage of the average relative absolute error (AAE) using the following formulae:

$$RMSE = \sqrt{\frac{1}{N} \sum_{i=1}^N (t_i - y_i)^2} \quad (2)$$

$$AAE = \frac{1}{N} \sum_{i=1}^N \left| \frac{t_i - y_i}{t_i} \right| \times 100 \quad (3)$$

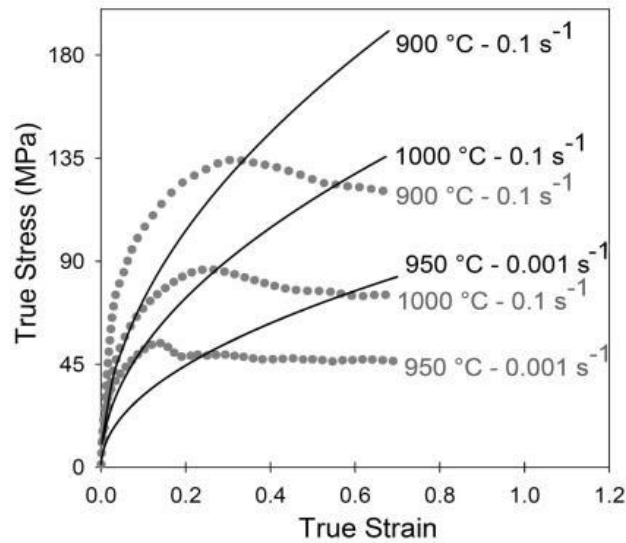


Fig. 3: Comparison between the experimental and the calculated flow curves by the original ZA model as expressed by Eq. 1.

where  $t_i$  is the target output,  $y_i$  is the model output, and  $N$  is the number of data points. The average RMSE and AAE were determined as 21.65 MPa and 37.88%, respectively. These high error values also confirm that the original ZA model is not appropriate for prediction of the hot flow stress. Due to the parabolic form of the strain-hardening term, the original ZA equation cannot represent the softening stage resulted from DRX. It can also be seen that it even fails to represent the hardening stage due to the adverse effect of the softening part of the flow curves on the obtained values of the constants of the ZA equation. Therefore, in the following sections, the modifications of the ZA model are being taken into account.

### 3.3. The ZA model with $n$ as a variable

The first imaginable modification is considering a power law strain hardening exponent of  $n$  instead of 0.5 to better account for the effect of DRV. The procedure for obtaining

the constants is similar to Section 3.2 and it is not included here for the sake of brevity. Only, obtaining  $n$  is presented. Once derived that  $B_1=0.00344 \text{ K}^{-1}$ , the ZA equation can be simplified as  $\ln \sigma = (\ln B_0 - 0.00344T) + n \ln \dot{\varepsilon}$ . It follows that the slope of the plot of  $\ln \sigma$  vs.  $\ln \dot{\varepsilon}$  at a constant temperature can be used to obtain the value of  $n$  at that specific temperature. This is shown in Fig. 4a. It can be seen that the lines are nearly parallel, and hence,  $n$  does not depend on temperature and its average value can be taken as 0.232, i.e. half the original exponent included in the ZA model. After obtaining all of the constants, the modified ZA equation can be expressed as follows:

$$\sigma = 6771.175 \dot{\varepsilon}^{0.232} \exp(-0.002953T + 0.00012T \ln \dot{\varepsilon}) \quad (4)$$

Fig. 4b shows the comparison between the experimental and calculated flow stress for some representative curves using Eq. 4. As it is apparent, the ZA model with  $n$  as a variable can better predict the hardening part of the flow curves but it cannot show the softening part. The average RMSE and AAE were determined as 10.03 MPa and 19.75%, respectively. These error values are lowering compared with the original ZA model, which confirm that the consideration of  $n$  values lower than 0.5 is a good modification. The main deficiency of this approach is behind the consideration of  $\beta_0$  as a constant. As can be seen in Fig. 5a,  $\beta_0$  considerably depends on strain. Therefore, it seems required to consider the strain dependency of  $\beta_0$ , which will be treated in Section 3.4.

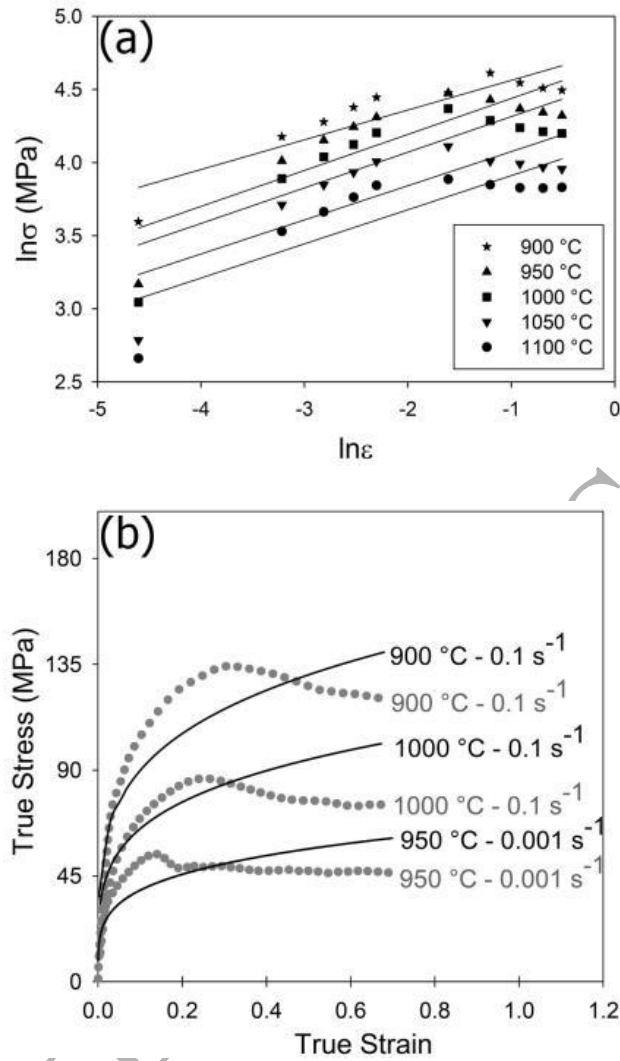


Fig. 4: Plot used for obtaining  $n$  along with the comparison between the experimental and the calculated flow curves by the ZA model as expressed by Eq. 4.

#### 3.4. The modification of ZA model by considering the flow softening

Based on the results of Section 3.3, the equation of  $\sigma = B_0 \epsilon^n \exp(-\beta_0 T + \beta_1 \ln \dot{\epsilon})$  with  $\beta_0$  as a function of strain (Fig. 5a) was considered in this section by fitting to a polynomial expression. Therefore, all other constants are the same as those determined in Section 3.3 and the modified ZA equation can be expressed as follows:

$$\sigma = 6771.175\varepsilon^{0.232} \exp(-\beta_0 T + 0.00012T \ln \dot{\varepsilon}) \quad (5)$$

$$\beta_0 = 0.0241\varepsilon^4 - 0.0364\varepsilon^3 + 0.0183\varepsilon^2 - 0.0027\varepsilon + 0.0029$$

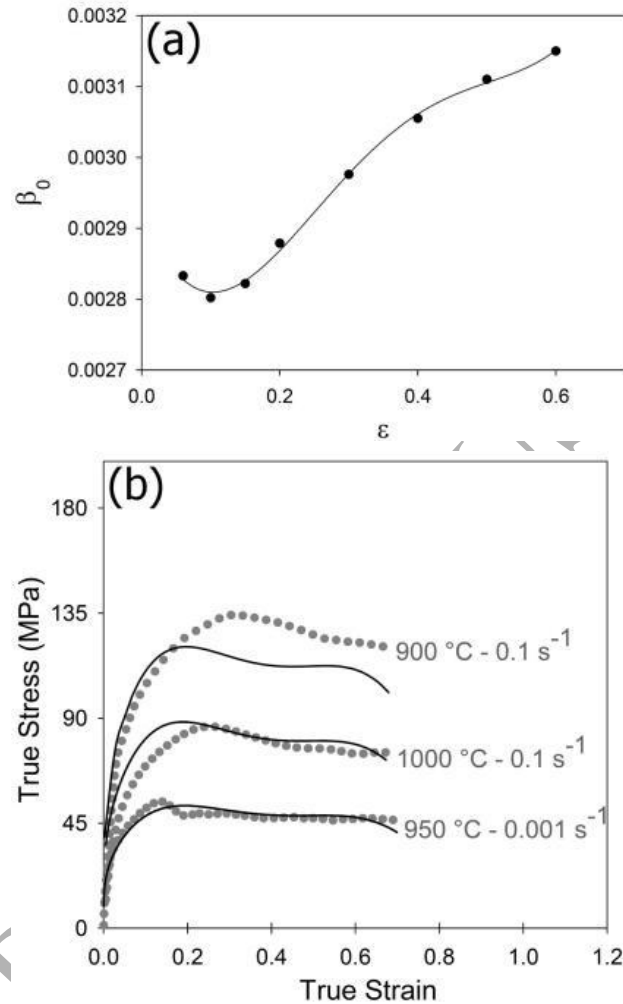


Fig. 5: Variation of  $\beta_0$  with strain along with the comparison between the experimental and the calculated flow curves by the ZA model as expressed by Eq. 5.

Fig. 5b shows the comparison between the experimental and calculated flow stress for some representative curves using Eq. 5. As it is apparent, Eq. 5 can predict the flow stress significantly better, especially it can represent the flow softening by DRX. It seems that the coupled effect of strain, strain rate, and temperature by considering the strain

dependency of  $\beta_0$  in  $\exp(-\beta_0 T + 0.00012T \ln \dot{\epsilon})$  can be achieved. The average RMSE and AAE were determined as 4.35 MPa and 9.45%, respectively. These low error values confirm the better applicability of Eq. 5 in modeling and prediction of flow stress. However, Fig. 5b shows that one of the problems of this approach is that the location of the peak point of the calculated flow curves does not match with that of the experimental flow curves. Another problem is evident from the steady-state part of the calculated flow curves. The former shows that it is required to consider the peak strain in analysis (this will be treated in Section 3.5) and the latter reveals that the consideration of  $\beta_0$  as a strain dependent variable has its own problems and the level of flow stress becomes very sensitive to the value of  $\beta_0$  as will be accounted for in Section 3.6.

### 3.5. The modification of ZA model by incorporation of peak strain

In the previous section, it was found that it is required to consider the peak strain in the analysis. Therefore, an equation of the form  $\sigma = B_0(\epsilon / \epsilon_p)^n \exp(-\beta_0 T + \beta_1 \ln \dot{\epsilon})$  is considered in this section.

For a given initial grain size, the classical power relation of  $\epsilon_p = pZ^q$  (Mirzadeh et al., 2010; Nazábal et al., 1987) can be employed to find a relation between the peak strain ( $\epsilon_p$ ) and the Zener-Hollomon parameter ( $Z = \dot{\epsilon} \exp(Q/RT)$ ) (Zener and Hollomon, 1944). Since the deformation mechanism during hot deformation is usually based on the glide and climb of dislocations, the lattice self-diffusion activation energy can be set as the deformation activation energy ( $Q$ ) (Mirzadeh et al., 2011a; Mirzadeh, 2014a). As a result, the lattice self-diffusion activation energy of austenite ( $Q_{SD} = 270$  kJ/mol) was considered here. Subsequently, the plot of  $\ln \epsilon_p$  vs.  $\ln Z$  was used to find the values of  $p$

and  $q$  as shown in Fig. 6 and the equation of  $\varepsilon_p = 0.0123Z^{0.125}$  was determined, which was used for calculating the values of peak strain for the subsequent analysis.

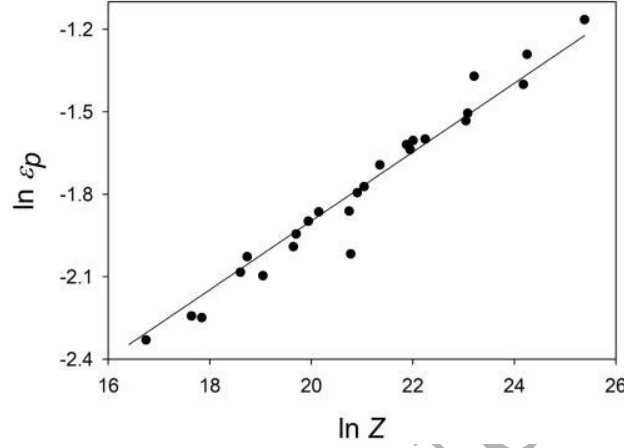


Fig. 6: The dependence of peak strain on the Zener-Hollomon parameter.

For obtaining the parameters of the model, the procedure of Section 3.4 was followed by consideration of  $\varepsilon/\varepsilon_p$  instead of  $\varepsilon$  and the dependency of  $\beta_0$  on  $\varepsilon/\varepsilon_p$  was considered (Fig. 7a). As a result, the following constitutive equation was determined:

$$\begin{aligned} \sigma &= 8757(\varepsilon/\varepsilon_p)^{0.233} \exp(-\beta_0 T + 0.00012T \ln \dot{\varepsilon}) \\ \beta_0 &= -0.0002(\varepsilon/\varepsilon_p)^3 + 0.0008(\varepsilon/\varepsilon_p)^2 - 0.0008(\varepsilon/\varepsilon_p) + 0.0036 \end{aligned} \quad (6)$$

Fig. 7b shows the comparison between the experimental and calculated flow stress for some representative curves using Eq. 6. As it is apparent, the problem at the peak point is amended but the problem of the steady-state part of the calculated flow curves becomes much worse. The average RMSE and AAE were determined as  $3.45 \times 10^{20}$  MPa and  $2.91 \times 10^{19}\%$ , respectively. These extremely large error values confirm that  $\beta_0$  should not be considered as a strain dependent variable. Also note that the polynomial fits in this

section and Section 3.4 were used in the range of experimental strain values and there is no guarantee that they will be satisfactory after extrapolation to higher strains.

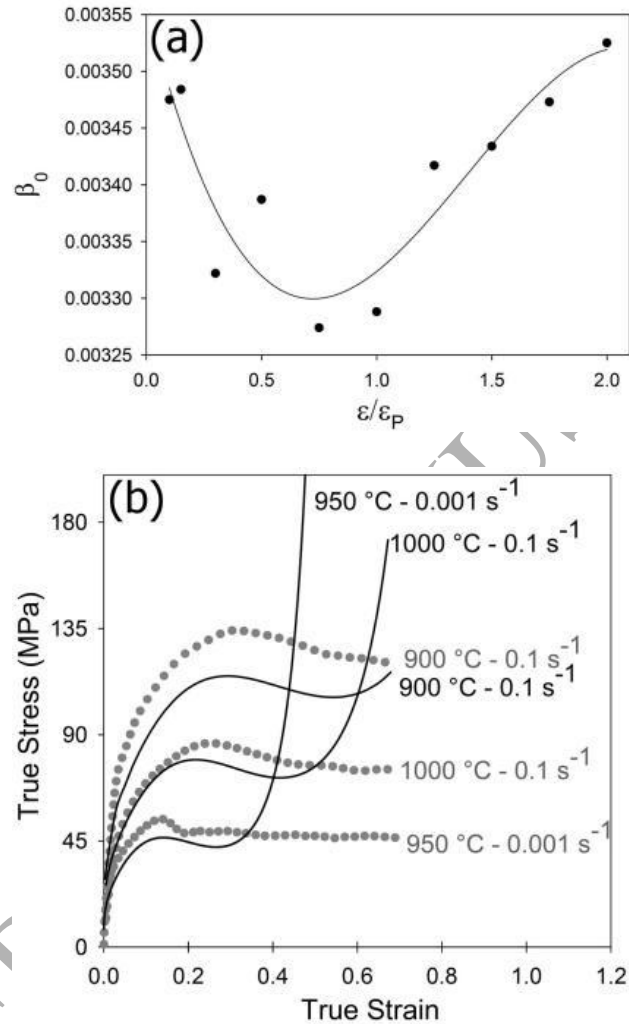


Fig. 7: Variation of  $\beta_0$  with strain along with the comparison between the experimental and the calculated flow curves by the ZA model as expressed by Eq. 6.

### 3.6. The proposed constitutive model

Based on the results of the previous sections, it was found that the strain hardening exponent of less than 0.5 can better account for the flow softening due to the DRV

process. Moreover, incorporation of the peak strain into the flow stress formula is a good modification to fix the problem at the peak point of flow curves. Furthermore, the consideration of  $\beta_0$  as a strain dependent variable is not the best choice. Also, based on Fig. 2b, it can be deduced that two slopes with different signs are actually required to represent the data due to flow hardening and softening stages. As a result, the following formula was considered as the appropriate modification of the ZA model:

$$\begin{aligned}\sigma &= B_{01}(\varepsilon/\varepsilon_p)^{n_1} \exp(-\beta_0 T + \beta_1 \ln \dot{\varepsilon}) \quad \text{if } \varepsilon \leq \varepsilon_p \\ \sigma &= B_{02}(\varepsilon/\varepsilon_p)^{n_2} \exp(-\beta_0 T + \beta_1 \ln \dot{\varepsilon}) \quad \text{if } \varepsilon \geq \varepsilon_p\end{aligned}\quad (7)$$

For calculating the appropriate value of  $B_{01}$ , the reference strain rate of  $0.03 \text{ s}^{-1}$  was considered again. It follows from  $\ln \sigma = \ln B_{01} + n_1 \ln(\varepsilon/\varepsilon_p) - (\beta_0 - \beta_1 \ln \dot{\varepsilon})T$  that the slope of the plot of  $\ln \sigma$  against  $T$  at a constant  $\varepsilon/\varepsilon_p$  can be used to obtain the value of  $B_1 = (\beta_0 - \beta_1 \ln \dot{\varepsilon}) = 0.00384 \text{ K}^{-1}$ . Based on the above analysis, the ZA equation can be simplified as  $\ln \sigma = (\ln B_{01} - 0.00384T) + n_1 \ln(\varepsilon/\varepsilon_p)$ . It follows that the slope and the intercept of the plot of  $\ln \sigma$  vs.  $\ln(\varepsilon/\varepsilon_p)$  at a constant temperature can be used to obtain the value of  $n_1$  and  $\ln B_{01} - 0.00384T$  at that specific temperature, respectively. This, along with the similar curve for  $B_{02}$  and  $n_2$ , is shown in Fig. 8a and the average values of  $n_1$ ,  $B_{01}$ ,  $n_2$ , and  $B_{02}$  were determined as 0.320, 9880.4 MPa, -0.173, and 9880.4 MPa, respectively. Note that based on Eq. 7, it was obvious that  $B_{01}$  should be equal to  $B_{02}$ . Finally, for calculating  $\beta_0$  and  $\beta_1$ , the similar procedure to the previous sections was used and the average values of  $\beta_0$  and  $\beta_1$  were determined as  $0.0034 \text{ K}^{-1}$  and  $0.00012 \text{ K}^{-1}$ , respectively. As a result, the following constitutive equation was determined:

$$\begin{aligned} \sigma &= 9880.4(\varepsilon / \varepsilon_p)^{0.320} \exp(-0.0034T + 0.00012 \ln \dot{\varepsilon}) \quad \text{if } \varepsilon \leq \varepsilon_p \\ \sigma &= 9880.4(\varepsilon / \varepsilon_p)^{-0.173} \exp(-0.0034T + 0.00012 \ln \dot{\varepsilon}) \quad \text{if } \varepsilon \geq \varepsilon_p \end{aligned} \quad (8)$$

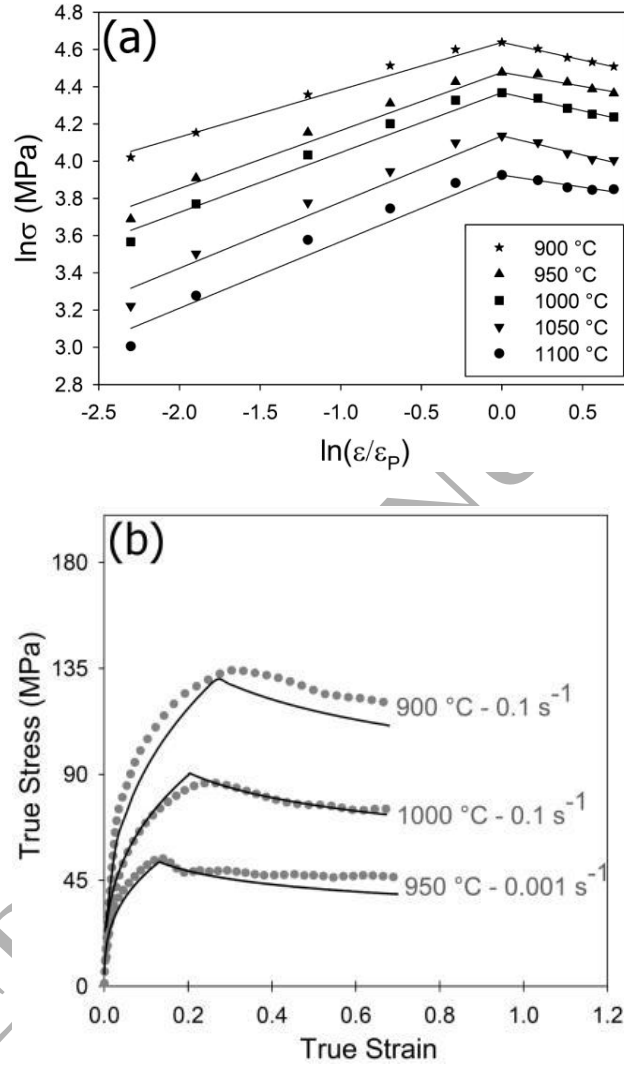


Fig. 8: Plot used for obtaining  $n_1$ ,  $B_{01}$ ,  $n_2$ , and  $B_{02}$  along with the comparison between the experimental and the calculated flow curves by the ZA model as expressed by Eq. 8.

Fig. 8b shows the comparison between the experimental and calculated flow stress for some representative curves using Eq. 8. As it is obvious, the proposed modified ZA model can be efficiently used for modeling and prediction of hot deformation flow

curves. The average RMSE and AAE were determined as 4.40 MPa and 10.14%, respectively. These error values are low and are comparable to those of the method described in Section 3.4 but the proposed method is superior because it can solve the problem of the location of the peak point of flow curves. However, an obvious drawback of the proposed method is behind the fact that it deals separately with the hardening and softening parts of the flow curve, and as a result, at the peak point, the modeled curves are not smooth. This might be a problem in process simulation. Anyway, the proposed constitutive equation can be conveniently and efficiently used to predict the hot flow stress while retaining the general form of the original physically-based ZA model. This model appropriately accounts for the effect of DRV and DRX at high temperatures and it is applicable to both of the hardening and softening parts of the flow curves.

#### 4. Conclusions

The applicability of the Zerilli-Armstrong (ZA) model for modeling and prediction of hot deformation flow stress was evaluated for alloys with FCC crystal structure and subsequently it was modified step-by-step to make it adaptable to high-temperature flow curves. The following conclusions can be drawn from this study:

(1) The original ZA model of the form of  $\sigma = c_0 + B_0 \varepsilon^{0.5} \exp(-\beta_0 T + \beta_1 T \ln \dot{\varepsilon})$  was not able to predict the softening part of the flow curves and it even failed to represent the hardening stage partly due to the adverse effect of the softening part on the obtained values of the constants. The latter shortcoming can be somehow amended by considering a power law strain hardening exponents of less than 0.5 to better account for the effect of DRV. The former problem can be treated by consideration of the strain dependency of

$\beta_0$  but in turn the location of the peak point of the calculated flow curves will not coincide with that of the experimental flow curves and the steady-state part of the calculated flow curves will become problematic.

(2) Incorporating the peak strain into the flow stress formula was found to be a good modification to fix the problem at the peak point of flow curves. However, the consideration of  $\beta_0$  as a strain dependent variable to account for the softening part of the flow curve will become a severe problem. It was also shown that two slopes with different signs are actually required to represent the data due to flow hardening and softening stages. As a result, the following useful formulas were proposed:

$$\sigma = B_0(\varepsilon / \varepsilon_p)^{n_1} \exp(-\beta_0 T + \beta_1 \ln \dot{\varepsilon}) \quad \text{if } \varepsilon \leq \varepsilon_p$$

$$\sigma = B_0(\varepsilon / \varepsilon_p)^{n_2} \exp(-\beta_0 T + \beta_1 \ln \dot{\varepsilon}) \quad \text{if } \varepsilon \geq \varepsilon_p$$

(3) While retaining the general form of the original physically-based ZA model, the proposed constitutive equation was found to be useful in prediction of hot flow stress. However, an obvious drawback of the proposed method is behind the fact that it deals separately with the hardening and softening parts of the flow curve, and as a result, at the peak point, the modeled curves are not smooth.

## References

Ahmed H., Wells M.A., Maijer D.M., Howes B.J., van der Winden M.R., Modelling of microstructure evolution during hot rolling of AA5083 using an internal state variable approach integrated into an FE model, *Materials Science and Engineering A* 390 (2005) 278-290.

- Akbari Z., Mirzadeh H., Cabrera J.M., A simple constitutive model for predicting flow stress of medium carbon microalloyed steel during hot deformation, *Materials and Design* 77 (2015) 126-131.
- Anand L., Constitutive equations for hot-working of metals, *International Journal of Plasticity* 1 (1985) 213-231.
- Cai J., Wang K., Zhai P., Li F., Yang J., Cai J., Wang K., Zhai P., Li F., Yang J., Modified Johnson-Cook constitutive equation to predict hot deformation behavior of Ti-6Al-4V alloy, *Journal of Materials Engineering and Performance* 24 (2015) 32-44.
- Chai R.X., Su W., Guo C., Zhang F., Constitutive relationship and microstructure for 20CrMnTiH steel during warm deformation, *Materials Science and Engineering A* 556 (2012) 473-478.
- Dehghan-Manshadi A., Barnett M.R., and Hodgson P.D., Hot deformation and recrystallization of austenitic stainless steel: Part I. dynamic recrystallization, *Metallurgical and Materials Transactions A* 39 (2008) 1359-1370.
- Doherty R.D., Hughes D.A., Humphreys F.J., Jonas J.J., Juul Jensen D., Kassner M.E., King W.E., McNelley T.R., McQueen H.J., Rollett A.D., Current issues in recrystallization: a review, *Materials Science and Engineering A* 238 (1997) 219-274.
- Escobar F., Cabrera J.M., Prado J.M., Effect of carbon content on plastic flow behavior of plain carbon steels at elevated temperature, *Materials Science and Technology* 19 (2003) 1137-1147.
- Johnson G.R., Cook W.H., A constitutive model and data for metals subjected to large strains, high strain rates and high temperatures, in: *Proceedings of the Seventh International Symposium on Ballistic*, The Hague, The Netherlands, 1983, 541-547.
- Langdon T.G., An Analysis of flow mechanisms in high temperature creep and superplasticity, *Materials Transactions* 46 (2005) 1951-1956.

- Lin Y.C., Xiao-Min Chen, A critical review of experimental results and constitutive descriptions for metals and alloys in hot working, *Materials and Design* 32 (2011) 1733-1759.
- Luo J., Li M., Li X., Shi Y., Constitutive model for high temperature deformation of titanium alloys using internal state variables, *Mechanics of Materials* 42 (2010) 157-165.
- Mirzadeh H., Najafizadeh A., Prediction of the critical conditions for initiation of dynamic recrystallization, *Materials and Design* 31 (2010) 1174-1179.
- Mirzadeh H., Najafizadeh A., Moazeny M., Hot deformation behaviour of precipitation hardening stainless steel, *Materials Science and Technology* 26 (2010) 501-504.
- Mirzadeh H., Cabrera J.M., Najafizadeh A., Constitutive relationships for hot deformation of austenite, *Acta Materialia* 59 (2011) 6441-6448.
- Mirzadeh H., Cabrera J.M., Prado J.M., Najafizadeh A., Hot deformation behavior of a medium carbon microalloyed steel, *Materials Science and Engineering A* 528 (2011) 3876-3882.
- Mirzadeh H., Cabrera J.M., Najafizadeh A., Calvillo P.R., EBSD study of a hot deformed austenitic stainless steel, *Materials Science and Engineering A* 538 (2012) 236-245.
- Mirzadeh H., Najafizadeh A., Hot deformation and dynamic recrystallization of 17-4 PH stainless steel, *ISIJ International* 53 (2013) 680-689.
- Mirzadeh H., Constitutive analysis of Mg–Al–Zn magnesium alloys during hot deformation, *Mechanics of Materials* 77 (2014) 80-85.
- Mirzadeh H., A comparative study on the hot flow stress of Mg–Al–Zn magnesium alloys using a simple physically-based approach, *Journal of Magnesium and Alloys* 2 (2014) 225-229.

Mirzadeh H., A simplified approach for developing constitutive equations for modeling and prediction of hot deformation flow stress, *Metallurgical and Materials Transactions A* 46 (2015) 4027-4037.

Mirzadeh H., Constitutive behaviors of magnesium and Mg–Zn–Zr alloy during hot deformation, *Materials Chemistry and Physics* 152 (2015) 123-126.

Mirzadeh H., Constitutive modeling and prediction of hot deformation flow stress under dynamic recrystallization conditions, *Mechanics of Materials* 85 (2015) 66-79.

Mirzadeh H., Quantification of the strengthening effect of reinforcements during hot deformation of aluminum-based composites, *Materials and Design* 65 (2015) 80-82.

Mirzadeh H., Constitutive Description of 7075 Aluminum Alloy During Hot Deformation by Apparent and Physically-Based Approaches, *Journal of Materials Engineering and Performance* 24 (2015) 1095-1099.

Mirzadeh H., Roostaei M., Parsa M.H., Mahmudi R., Rate controlling mechanisms during hot deformation of Mg–3Gd–1Zn magnesium alloy: Dislocation glide and climb, dynamic recrystallization, and mechanical twinning, *Materials and Design* 68 (2015) 228-231.

Mukherjee A.K., An examination of the constitutive equation for elevated temperature plasticity, *Materials Science and Engineering A* 322 (2002) 1-22.

Nazábal J.L., Urcola J.J., Fuentes M., The transition from multiple- to single-peak recrystallization during the hot working of austenite, *Materials Science and Engineering*, Volume 86 (1987) 93-103.

Parsa M.H., Ohadi D., A constitutive equation for hot deformation range of 304 stainless steel considering grain sizes, *Materials and Design* 2 (2013) 412-421.

Saadatkia S., Mirzadeh H., Cabrera J.M., Hot deformation behavior, dynamic recrystallization, and physically-based constitutive modeling of plain carbon steels, *Materials Science and Engineering A* 636 (2015) 196-202.

Samantaray D., Mandal S., Borah U., Bhaduri A.K., Sivaprasad P.V., A thermo-viscoplastic constitutive model to predict elevated-temperature flow behaviour in a titanium-modified austenitic stainless steel, *Materials Science and Engineering A* 526 (2009) 1-6.

Sun Z.C., Yang H., Han G.J., Fan X.G., A numerical model based on internal-state-variable method for the microstructure evolution during hot-working process of TA15 titanium alloy, *Materials Science and Engineering A* 527 (2010) 3464-3471.

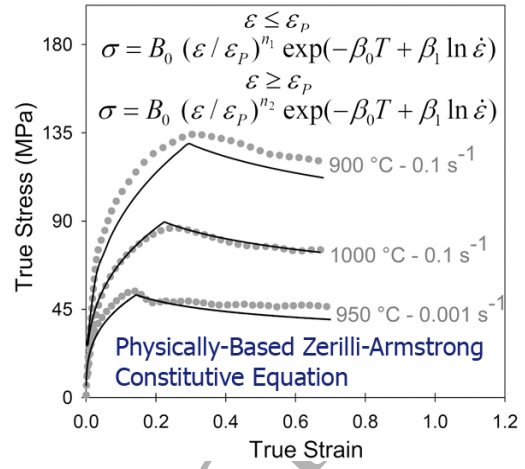
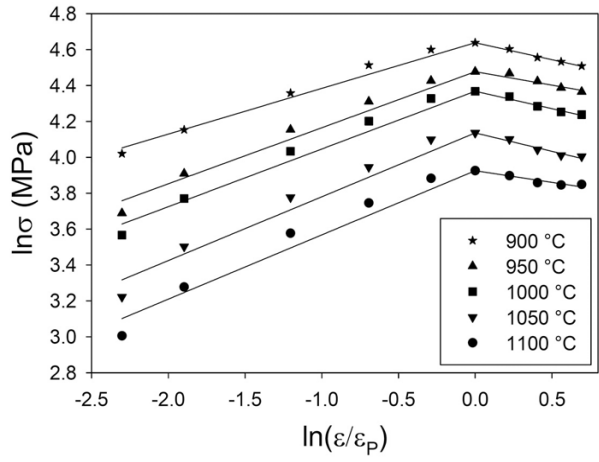
Zener C., Hollomon J.H., Effect of strain rate upon plastic flow of steel. *Journal of Applied Physics* 15 (1944) 22-32.

Zerilli F.J., Armstrong R.W., Dislocation-mechanics-based constitutive relations for material dynamics calculations, *Journal of Applied Physics* 61 (1987) 1816-1825.

Zerilli F.J., Dislocation mechanics–based constitutive equations, *Metallurgical and Materials Transactions A* 35 (2004) 2547-2555.

Zhang H., Wen W., Cui H., Xu Y., A modified Zerilli–Armstrong model for alloy IC10 over a wide range of temperatures and strain rates, *Materials Science and Engineering A* 527 (2009) 328-333.

## Graphical abstract



ACCEPTED MANUSCRIPT